Ab Initio Wavenumber Accurate Spectroscopy: $^1CH_2$ and HCN Vibrational Levels on Automatically Generated IMLS Potential Energy Surfaces†

Richard Dawes,‡ Albert F. Wagner,§ and Donald L. Thompson*,‡

Department of Chemistry, University of Missouri—Columbia, Columbia, Missouri 65211, and Chemistry Division, Argonne National Laboratory, Argonne, Illinois 60439

Received: January 14, 2009; Revised Manuscript Received: February 4, 2009

We report here calculated $J = 0$ vibrational frequencies for $^1CH_2$ and HCN with root-mean-square error relative to available measurements of 2.0 cm^{-1} and 3.2 cm^{-1}, respectively. These results are obtained with DVR calculations with a dense grid on ab initio potential energy surfaces (PESs). The ab initio electronic structure calculations employed are Davidson-corrected MRCI calculations with double-, triple-, and quadruple-ζ basis sets extrapolated to the complete basis set (CBS) limit. In the $^1CH_2$ case, Full CI tests of the Davidson correction at small basis set levels lead to a scaling of the correction with the bend angle that can be profitably applied at the CBS limit. Core-valence corrections are added derived from CCSD(T) calculations with and without frozen cores. Relativistic and non-Born—Oppenheimer corrections are available for HCN and were applied. CBS limit CCSD(T) and CASPT2 calculations with the same basis sets were also tried for HCN. The CCSD(T) results are noticeably less accurate than the MRCI results while the CASPT2 results are much poorer. The PESs were generated automatically using the local interpolative moving least-squares method (L-IMLS). A general triatomic code is described where the L-IMLS method is interfaced with several common electronic structure packages. All PESs were computed with this code running in parallel on eight processors. The L-IMLS method provides global and local fitting error measures important in automatically growing the PES from initial ab initio seed points. The reliability of this approach was tested for $^1CH_2$ by comparing DVR-calculated vibrational levels on an L-IMLS ab initio surface with levels generated by an explicit ab initio calculation at each DVR grid point. For all levels ($\sim$200) below 20 000 cm^{-1}, the mean unsigned difference between the levels of these two calculations was 0.1 cm^{-1}, consistent with the L-IMLS estimated mean unsigned fitting error of 0.3 cm^{-1}. All L-IMLS PESs used in this work have comparable mean unsigned fitting errors, implying that fitting errors have a negligible role in the final errors of the computed vibrational levels with experiment. Less than 500 ab initio calculations of the energy and gradients are required to achieve this level of accuracy.

1. Introduction

The small size of singlet methylene ($^1CH_2$) and hydrogen cyanide (HCN) has made them accessible to high level electronic structure calculations for more than 20 years. The vibrational eigenstates of each molecule continue to hold the interest of theoreticians and experimentalists, although for different reasons. The pioneering high level ab initio-based calculations of the vibrational levels were done by Green et al.[1] and Comeau et al.[2] for $^1CH_2$ around 1990 and compared to experimental results.[3–45] Singlet CH_2 has a Renner—Teller coupling which received attention then[6,7] and in more recent times.[8–16] In a series of papers Bowman and co-workers[17–22] compared computed vibrational levels for HCN to values derived from measurements.[23–28] Additional experimental results[29–31] also became available. More recently van Mourik et al.[32] have calculated vibrational levels with a higher quality potential energy surface (PES). Quite recently Varandas et al.[33] has empirically adjusted a PES based on ab initio calculations to closely reproduce the experimental vibrational levels. The HCN:HNC system has been widely used for studying isomerization.[20,34,35]

The electronic structure methods used in those studies have been either multireference configuration interaction (MRCI) or coupled cluster methods. The earlier work by Green et al.,[1] Comeau et al.,[2] and Bowman et al.[17–22] did not use large basis sets by today's standards while van Mourik et al.[32] incorporated some results calculated with a very large five zeta basis set. In all cases, the comparison between measured vibrational levels and ab initio vibrational levels (with no empirical corrections) showed root-mean-square (rms) errors in the range of 10 to 60 cm^{-1}. These errors are small enough to allow a confident assignment of vibrational levels but they are very much larger than the uncertainty in the measured levels. For such small molecules, can we further reduce the error?

The calculated vibrational levels are produced by quantum eigenstate calculations on a continuous PES fit to energies calculated at discrete geometries by an electronic structure method. While at a fine level of comparison, relativistic effects, non-Born—Oppenheimer effects, and inaccuracies in the quantum dynamics calculation all produce errors, typically such errors are small relative to deficiencies in the electronic structure method and in the fitting methods.[36] The electronic structure methods used in the studies discussed above have basis set incompleteness errors and intrinsic correlation errors. None of these past studies used complete basis set (CBS) extrapolation techniques in which results from a series of basis sets are

† Part of the "George C. Schatz Festschrift" Special Issue.

* Corresponding author. E-mail: thompsondon@missouri.edu.
‡ University of Missouri—Columbia.
§ Argonne National Laboratory.

10.1021/jp900409r CCC: $40.75
Published on Web 03/16/2009

extrapolated to an infinite basis limit as an approximate means of eliminating the basis set error over the entire PES. Correlation error is more difficult in practice to approach systematically. However, contrasting MRCI and coupled cluster techniques at the same basis set level or contrasting MRCI calculations with or without the Davidson correction or with the simpler CASPT2 approximations to the MRCI approach are ways to alter how correlation is treated. Sensitivity of vibrational levels to these changes can be a measure of the significance of correlation error. In this paper, we address these issues for HCN and $^1CH_2$.

The methods used to fit ab initio data to obtain the PESs used in those studies also present possibilities for errors. The fitting methods employed in the studies are based on functional forms with parameters adjusted by least-squares to the calculated energies at a set of discrete geometries. The error of these fits was not systematically determined, but preliminary tests of various sorts suggested that the errors were small. Most spectroscopic quality fitted PESs have been developed in a similar way and require considerable human effort and often application-specific physically motivated fitting functions.[37–39] However, in recent years a number of fitting methods have been developed that have the potential of fitting the calculated energies with higher accuracy, more efficiency, and with more systematic control over fitting error. These methods include interpolating moving least squares (IMLS),[40–42] splines,[43–46] modified-Shepard (MS) interpolation,[47–49] neural networks (NN),[50–58] reproducing kernel Hilbert space (RKHS),[59,60] and Morse function polynomials.[61–63] In the present study we used IMLS-based methods for generating HCN and $^1CH_2$ PESs because they give a measure of the fitting error, seamlessly incorporate gradients from electronic structure calculations, and select the discrete geometries at which electronic structure calculations will optimize the convergence of the fit. The results show that IMLS fitting methods *enable* more expensive higher level electronic structure calculations because, relative to other fitting methods, far fewer such calculations are needed for a converged fit to higher accuracy.

The rest of the paper is arranged as follows. In section 2 we discuss the methods used, with the primary focus being on the IMLS fitting method and its marriage to several electronic structure code packages. Details of how we calculate vibrational levels for a PES will also be discussed. In section 3 we present results for $^1CH_2$ and HCN:HNC. These results will primarily feature vibrational level calculations for the $J = 0$ band origins and comparison of these to measurements and past theoretical calculations. A summary and the conclusions are given in section 4.

2. Methods

A. Surface Fitting and Electronic Structure. Previously we have demonstrated a general method for fitting PESs based on IMLS fits to ab initio data stored at a limited number of local expansion points (L-IMLS).[40–42] The method has the flexibility to fit (1) energies, (2) energies and gradients, or (3) energies, gradients, and Hessians. The fit is continuous and provides analytic gradients. The method permits fully automated PES generation. Beginning with an initial set of seed points, an automatic point selection scheme determines where new data are required and, in a series of iterations, computes new ab initio data and updates the fit until the specified accuracy is reached, which is achieved with many fewer ab initio points than most other methods. To determine locations for new points, the data are fit using two successive degrees of the fitting basis set, and the negative of the squared difference between the two fits provides a differentiable continuous surface whose minima determine locally optimal locations for new ab initio points. This difference surface will never have a minimum very near an existing data point because the IMLS fit always goes through each data point no matter what basis set is used, making the difference surface zero at all data points already included in the fit.

In most of our previous studies, in which the focus was the development of the method, we refit published analytical surfaces[40–42] over ranges of energies and coordinates to get global PESs. In the present study we have interfaced this fitting approach to three popular electronic structure codes (Gaussian,[64] Aces II,[65] and Molpro[66]) to automatically generate new ab initio PESs. The result is a three-atom code that can be used to generate a new PES for any three-atom system to a specified accuracy over specified ranges of energy and coordinates. The code has automatic symmetry recognition and allows the user to select from a variety of coordinates and electronic structure methods. The code runs in parallel and all the calculations in this paper were run on eight parallel processors. A more detailed description of this code and its availability is contained in Supporting Information in the form of an Appendix. Because of its impact on this current work and because it has not been used in our previous studies, there is one feature of the code we briefly describe here which is more fully described in the Supporting Information. As mentioned above, the search for the optimal location of the next ab initio point requires the code to find the global minimum in the negative squared difference surface. As the Supporting Information details, the number of local minima grow with the number of included ab initio points in the fit. Our previous searches used a fixed number of random starting points for the minimization search, a strategy that does not grow with the number of ab initio points. The code we use here uses both a fix number of random starting points and a collection of midpoints between already included points. because that collection grows with the number of included points, the new code performs a more comprehensive search for the location of the next ab initio point to include, thereby accelerating the convergence of the fit.

In applying this code to the generation of $^1CH_2$ and HCN PESs, we monitored the results in two ways. First, as mentioned in the Supporting Information, electronic structure calculations do not always converge to the ground state. Fitting a PES to a data set containing several improperly converged points poses obvious problems. As the surfaces were being produced, we monitored the results, especially those involving high symmetry linear geometries (specifically discussed in the Supporting Information). We believe the electronic structure calculations used in the fits were all properly converged. Second, the code measures fitting error in terms of the difference surface between two fits, each with a different basis set (as described briefly above and in more detail in the Supporting Information). To confirm how effective the difference surface is as an error estimator, we performed a test set of 500 new ab initio calculations every 10 iterations for the less expensive electronic structure calculations. These ab initio points were chosen randomly from a uniform distribution over each coordinate range, and error statistics of these 500 points with respect to the larger basis set L-IMLS fit is a measure of the true fitting error. This true error can then be compared to the corresponding difference error to assess the reliability of the latter in measuring the accuracy of the fit. The results strongly support the usefulness of the difference error, confirming our finding in previous studies.[40,42] This is discussed in section 3.

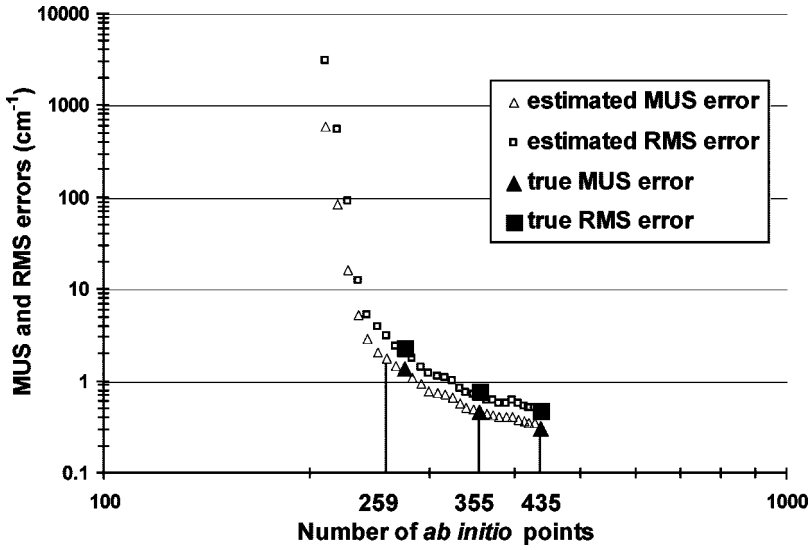

Figure 1. Convergence of IMLS automatic surface generation ($^1CH_2$, valence coordinates) to subwavenumber accuracy. Test sets of 8000 randomly placed points were used to evaluate rms (unfilled squares) and mean unsigned (unfilled triangles) estimated errors. Test sets of 500 randomly placed ab initio points were used to evaluate rms (filled squares) and mean unsigned (filled triangles) true errors. PES data files were outputted for vibrational calculations (Figure 4) at estimated mean unsigned errors of (A) 2.0 cm^{-1} (259 data points), (B) 0.5 cm^{-1} (355 data points), and (C) 0.33 cm^{-1} (435 data points).

B. Vibrational Levels. We calculated the vibrational levels using the Discrete Variable Representation (DVR) method.[67,68] A Potential-Optimized DVR (PODVR)[69,70] was used to describe each of the stretching coordinates (Radau for $^1CH_2$ and Jacobi for HCN) while a Legendre DVR was used to describe the bend in both $^1CH_2$ and HCN. For $^1CH_2$, 22 points were used for each stretching coordinate and 50 points were used for the bend, for a total of 22 400 points ($22 \times 22 \times 50$) in the DVR calculation. We computed all of the vibrational $J = 0$ band origins up to $\sim$20 000 cm^{-1} from the bottom of the well. For HCN, 50 points were used in each coordinate for a total of 125 000 points. This was more than sufficient for convergence of all the computed levels to an error very much smaller than that caused by the limitations of the underlying electronic structure calculations and the fitting procedure.

3. Results and Discussion

We used expensive high level electronic structure calculations to compute geometries and vibrational levels for $^1CH_2$ and HCN directly comparable to experiment. It is essential that the fitting error involved in constructing the PESs have an inconsequential effect on the comparisons and that the number of ab initio points required for the fit be as small as possible. To this end, we have run for both $^1CH_2$ and HCN preliminary less expensive electronic structure calculations that document the efficiency and the accuracy of the IMLS procedure for constructing the PESs. Because $^1CH_2$ is the simpler system, our test runs for it were more extensive. We present first these fitting accuracy tests followed by discussions of the highest quality calculations for $^1CH_2$ and HCN.

A. $^1CH_2$. ***Fitting Accuracy Tests.*** For our preliminary tests, the Molpro code was used to compute energies and gradients for the CASSCF (full valence) method using the relatively inexpensive aug-cc-pVDZ basis set. In constructing a PES, there is always the question of what coordinates to use. Because the degree of coupling depends on the coordinates, how efficiently a PES can be constructed from ab initio calculations is coordinate dependent. For $^1CH_2$, we tested both valence and bond distance coordinates.

For valence coordinates, the fit extended over ranges for r_{CH1} and r_{CH2} (C−H distances) of 0.78 Å to 2.55 Å, and θ (H−C−H angle) from 28° to 180°. The energy range was set to 20 000 cm^{-1}. The IMLS fitting basis used here and for all the calculations in this paper was of the High Dimensional Model Representation (HDMR) form,[71] specifically HDMR(12,9,7), which we have found useful in other studies.[40–42] The convergence behavior of the fit is shown in Figure 1. Starting with 211 seed points, the automatically generated points allowed rapid convergence of the fit with estimated and true errors (see Section 2) in close agreement. Data files for use of the fitted PESs were generated when the 2.0, 0.5, and 0.33 cm^{-1} estimated mean unsigned error (MUSE) accuracy targets were reached, which were met with 259, 355, and 435 symmetry unique ab initio points, respectively. The three fitted surfaces were used in variational vibrational calculations, which are described below.

A similar fit was done in bond distance coordinates. The ranges of coordinates were chosen to make the configuration spaces as similar as possible. The two C−H bond distances ranged from 0.78 Å to 2.55 Å just as in the valence coordinates fit. The H−H distance was allowed to range from 0.51 Å to 5.10 Å. The maximum H−H distance allows linear configurations for all C−H distances just as the maximum angle of 180° does in valence coordinates. Unavoidably, for the longest C−H bond distance values, the minimum H−H distance produced H−C−H angles ($\sim$11.5°) that were less than the minimum angle in the fit with valence coordinates. The energy range was again set to 20 000 cm^{-1}. Beginning with 153 seed points, convergence of the automatically generated surface was fairly rapid but certainly not as good as with the valence coordinates. As shown in Figure 2, the estimated MUSE reached about 2.8 cm^{-1} before the PES generation was terminated at 500 symmetry unique points. The valence coordinate fit was below that accuracy level with only 259 points. This is due to both the slightly larger configuration space included in the fit with bond distance coordinates, as well as stronger coordinate couplings in the bond distance description. As a consequence of these results, bond coordinates were not used further in the $^1CH_2$ or HCN calculations.

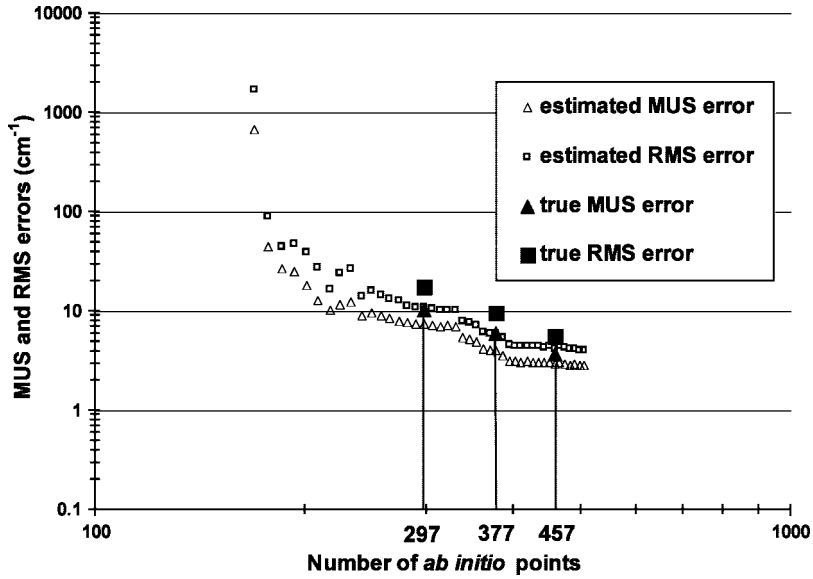

Figure 2. As in Figure 1 but for bond distance coordinates.

All the fitted surfaces discussed above have estimated and true errors established by large test sets of random points. For the valence coordinate fits to three different accuracies (2.0, 0.5, and 0.33 cm^{-1}), we tested how these errors would be reflected in a typical DVR spectroscopic calculation of the vibrational levels. Vibrational levels computed by using the fitted surfaces were compared to vibrational levels computed on the exact ab initio surface. In other words, a vibrational calculation was done using direct ab initio quadrature, for which an ab initio calculation was performed at each of the 22 400 points required by the DVR. Using the same electronic structure methods employed to fit the PES, the direct ab initio DVR calculation produced 216 bound vibrational states within the 20 000 cm^{-1} energy range. On all three fitted surfaces there were also exactly 216 bound vibrational states below 20 000 cm^{-1}. Figure 3 shows the errors relative to the direct ab initio results for each of the 216 states computed using the three surfaces (surfaces A, B, and C with an estimated fitting MUSE of 2.0, 0.5, and 0.33 cm^{-1}, respectively). The MUSE in the 216 vibrational levels computed using surface A with 259 data points (estimated 2.0 cm^{-1} fitting MUSE) is only 0.36 cm^{-1}. However, two of the higher energy levels have a much larger error than the rest, and thus the maximum error is 6.63 cm^{-1}. The levels computed using surface B (355 data points and 0.5 cm^{-1} estimated fitting MUSE) are much more accurate with MUSE and maximum errors of 0.14 and 0.72 cm^{-1}, respectively. Finally we tested surface C that includes 435 ab initio points and achieved a fitting MUSE of only 0.33 cm^{-1}. MUSE and maximum errors of 0.10 and 0.41 cm^{-1}, respectively, over the 216 vibrational levels is superb agreement with the exact surface. It is noteworthy that the error in the results shown in Figure 3 is very evenly distributed across the energy range. Our new exhaustive search strategy for optimal data point locations (see section 2.A and Supporting Information) is unbiased and searches strictly for maximal estimated error regardless of location. Also the fit is flexible in all regions because it is composed of a large number of local expansions rather than a single expansion about a minimum. In contrast, some fitting methods are designed around a single expansion point and thus tend to fit PESs most accurately at the bottom of a well with the fit worsening with increasing energy.

The overall results of these preliminary tests is that using valence coordinates and IMLS automatic surface generation produces with 400−500 points PESs with fitting errors reliably estimated by the IMLS method and with resulting errors in the computed levels well below 1 cm^{-1}. As comparisons of high quality electronics structure calculations with experiments discussed below show, this level of fitting error is inconsequential is assessing the difference between high quality theory and experiment.

High Quality Surfaces: $^1CH_2$. Having established the accuracy of the IMLS fitting method and the fidelity of computed vibrational levels for $^1CH_2$ using low-level ab initio calculations, a series of high-quality surfaces were then computed. Several PESs for $^1CH_2$ exist in the literature with which comparisons could be made. We will not compare to the empirically adjusted PESs that have been reported, but we confine our comparisons to purely ab initio PESs. Consequently, we will not compare to the most recent theoretical work on the $\tilde{a}\ ^1A_1$ lowest singlet CH_2, that by Duxbury et al.[9] who focused on the Renner−Teller coupling for ro-vibrational states with $K > 0$ but did not compute an ab initio PES. Here we focus on the $J = 0$ levels and compare to those calculated by Green et al.[1] and Comeau et al.[2] using fitted ab initio PESs for this state. They used physically motivated fitting functions, a minimal number of parameters, and a corresponding minimal number of electronic structure calculations (158 energy only calculations for Green et al. and 24 energy only calculations for Comeau et al.). They both fit to MRCI energies, while Comeau et al. also separately fit to Davidson-corrected (MRCI+Q) points. For most vibrational levels, Comeau et al. recorded better agreement with experiment using the fit without the Davidson correction (MRCI).

To develop a higher quality PES, we used the augmented triple- and quadruple-ζ basis sets (aug-cc-pVTZ and aug-cc-pVQZ). Extrapolation to CBS was performed using[72]

$$E(X) = E(\infty) + AX^{-3} \tag{1}$$

as well as with a three-parameter mixed Gaussian and exponential formula[73]

$$E(n) = E_{CBS} + b\exp[-(n-1)] + c\exp[-(n-1)^2] \tag{2}$$

Additional surfaces were computed using the aug-cc-pVDZ basis to incorporate into eq 2. To assess the value of the Davidson

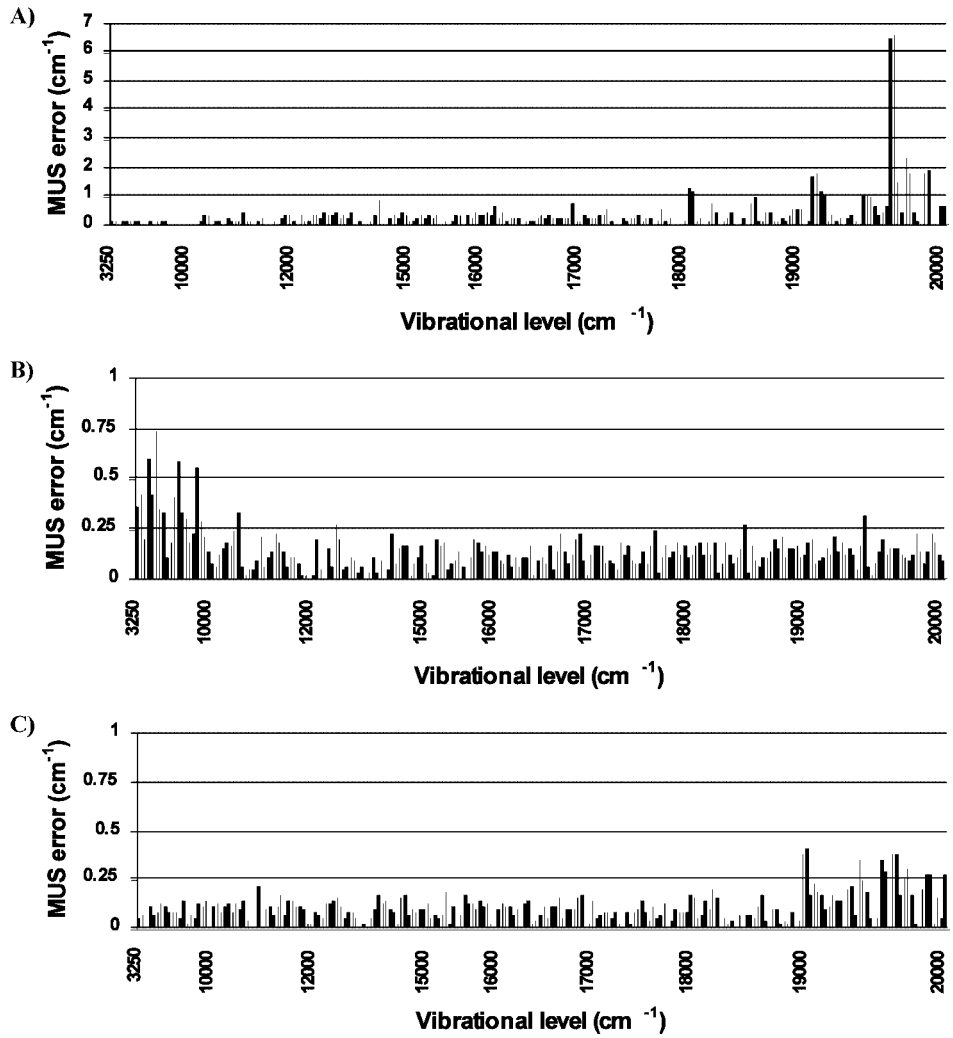

Figure 3. Plot of mean unsigned errors for 216 vibrational levels (below 20 000 cm^{-1}). Variational vibrational calculations were performed using a DVR approach on fitted PESs with estimated mean unsigned fitting errors of (A) 2.0 cm^{-1}, (B) 0.5 cm^{-1}, and (C) 0.33 cm^{-1}. The MUS errors in the plot are with respect to the exact levels determined by the same DVR calculation using ab initio calculations at all 22400 DVR points. The ab initio calculations are at the CASSCF/aug-cc-pVDZ level.

correction, we performed separate fits to both the MRCI and MRCI+Q methods. Based on vibrational calculations (discussed later), CBS extrapolation using eq 1 (and $X = 3, 4$) was deemed to be slightly more accurate than results obtained using eq 2 and including a double-ζ surface. Thus, only CBS results using eq 1 for $^1CH_2$ are discussed further. The Molpro code[66] was used to compute energies and gradients for the MRCI and MRCI+Q methods using a full-valence CASSCF reference. A core-valence correction surface was also computed using the difference between two separately fit surfaces at the CCSD(T)/aug-cc-pCVTZ level of theory (all-electrons correlated and frozen core). The equilibrium geometric parameters for the fitted surfaces are given in Table 1. Because the IMLS fitting method passes through all data points it is possible to ensure that the minima or barriers of the fitted surface correspond precisely with those of the ab initio method (by including data at those points). We did not add special points in this case, but the overall fitting accuracy nevertheless produces results in precise agreement with separate ab initio geometry optimizations. As shown in Table 1, at the CBS limit, both the MRCI and the Davidson-corrected surface agree well with the experimental values.[74] The two methods predict essentially the same bond distance while the Davidson correction improves the calculated angle slightly. The addition of the core-valence correction shortens the calculated distance slightly. We note that we are reporting the minima of the PES whereas the experiments measure the expectation value of the coordinate in the ground vibrational state. Because the ground-state vibrational wave function slightly favors coordinate deviations from equilibrium in the less steeply varying regions of the PES, the experimental expectation values for distance and the angle should, if anything, be larger than our computed values, as found in Table 1.

TABLE 1: Basis Set and ab Initio Method Dependence of Equilibrium Geometric Parameters for $^1CH_2$ (lowest singlet electronic state: $\tilde{a}\ ^1A_1$) on IMLS Fitted Surfaces

method/basis	r_{CH}/Å	θ/deg
aug-cc-pVTZ/MRCI	1.1109	101.90
aug-cc-pVQZ/MRCI	1.1090	102.03
CBS_1/MRCI	1.1076	102.12
CBS_1/MRCI+CV	1.1062	102.17
aug-cc-pVTZ/MRCI+Q	1.1109	102.05
aug-cc-pVQZ/MRCI+Q	1.1089	102.19
CBS_1/MRCI+Q	1.1076	102.27
expt.[a]	1.107	102.4

[a] Petek et al.[74]

Figure 4 shows a slice through the potential for each of the bases and methods. The slice is a scan of one stretching coordinate while the other bond distance and angle are held

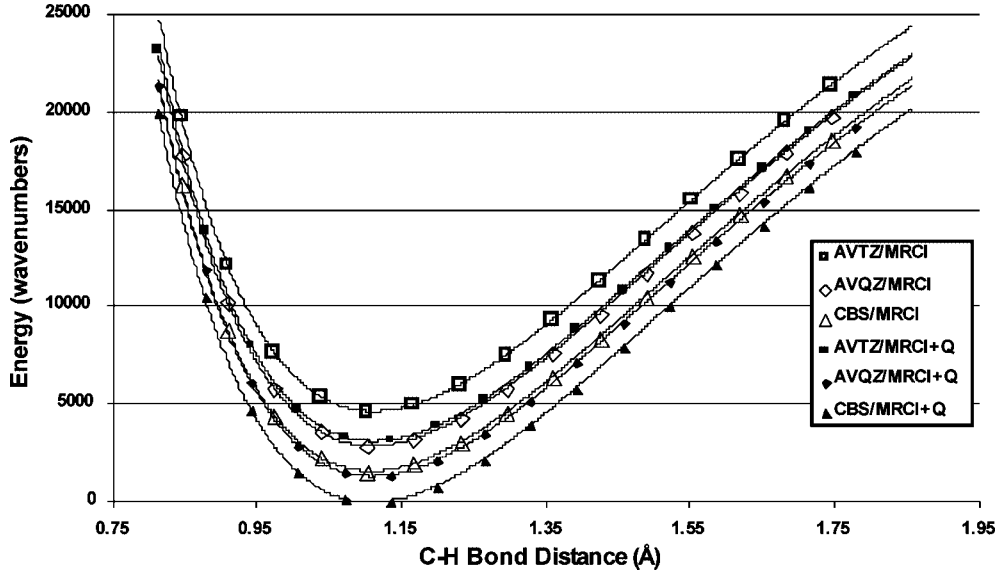

Figure 4. Slices though IMLS-based PESs for $^1CH_2$. Slices are a scan of one C−H bond distance with the other bond distance and angle held fixed at equilibrium values. Augmented triple- and quadruple-ζ bases are extrapolated to CBS limit (see text).

fixed at their equilibrium values. It is clear that a smooth, well-behaved fit results from the weighted sum of high-degree local expansions used in the IMLS method. The curves for the MRCI and MRCI+Q methods are qualitatively similar, with a shift toward a shorter equilibrium bond distance occurring with increasing basis set. As seen in Figure 4, the Davidson correction from an energy perspective is approximately equivalent to an increase of 1 in the zeta level of the basis set.

Table 2 compares calculated vibrational levels with ab initio-based results available in the literature as well as with experiment. Our high-level vibrational calculations were performed the same way as the test calculations described above. Barclay et al.[7] published a compilation of calculated and experimental results for the first 30 levels of this system. They include the results of a DVR calculation on the ab initio PES of Comeau et al.[2] We have reproduced those results and added the results reported by Green et al.[1] for their unadjusted ab initio surface. All of the IMLS fitted surfaces were found to be physically realistic and accurate. Green et al. calculations are only available for seven experimental levels. The rms errors with respect to those seven levels are as follows: Green et al. (12.4 cm^{-1}), CBS/MRCI (8.6 cm^{-1}), and CBS/MRCI+Q (9.7 cm^{-1}). Comeau et al. are available for 11 experimental levels, for which the rms errors are as follows: Comeau et al. (56.3 cm^{-1}), CBS/MRCI (10.7 cm^{-1}), and CBS/MRCI+Q (22.5 cm^{-1}). With regard to all 13 experimental levels, the rms error for our results are as follows: CBS/MRCI (10.7 cm^{-1}) and CBS/MRCI+Q (20.8 cm^{-1}). Addition of the core-valence correction to the CBS/MRCI surface improved several levels, but worsened others, with a net result of 11.29 cm^{-1} rms error. Notably the stretching modes are improved while the bending levels are worsened.

Within the experimental data there are two progressions with three or more members, i.e., $(0,v,0)$ and $(1,v,0)$. Relative to experiment, the CBS/MRCI+Q results are too anharmonic and consistently undershoot the experimental values by amounts that tend to grow quadratically with v. On the other hand, the CBS/MRCI results are not anharmonic enough and overshoot the experimental values but by an amount that tends to grow more linearly with v. To better understand the performance of the MRCI method and effect of the Davidson correction in this system with respect to valence correlation, we performed full CI benchmark calculations at a few points using small basis sets (6−31G*, cc-pVDZ, aug-cc-pVDZ, and cc-pVTZ). As expected from our vibrational calculations at the MRCI and MRCI+Q CBS limits, the Davidson correction was found to increasingly overcorrect the energy (relative to full CI) as a function of bond angle. On the basis of these results, we created two new surfaces with scaled Davidson corrections (vibrational results in Table 2). The scaling parameters are derived from small basis MRCI and Full CI results and then applied to surfaces extrapolated to a CBS limit. The two surfaces are denoted MRCI/CBS+CV+W(Q) and MRCI/CBS+CV+DW(Q). The first applies a constant scaling factor to the Davidson correction (chosen to approximate full CI around the equilibrium geometry). This produces a noticeable improvement, lowering the rms error from 11.29 to 8.84 cm^{-1}. Because this does not compensate for the quadratic nature of the Davidson overcorrection, the higher bend levels are still in larger error. For the second, a dynamically weighted Davidson correction was applied (quadratic in bond angle). With this simple correction the rms error in the vibrational levels was further reduced by more than a factor of 4 to 1.95 cm^{-1}.

Our conclusions are that for $^1CH_2$, CBS/MRCI based on an augmented triple- and quadruple-ζ extrapolation produces results via an L-IMLS PES in significantly better agreement with experiment than the past results of either Green et al. or Comeau et al. The Davidson correction overcorrects (relative to full CI) at the small basis set level and degrades agreement with experiment at the CBS level. Comeau et al. also concluded that the Davidson correction was not advisable, consistent with other observations of its limitations for few electron systems,[75–77] including CH_2.[78] With the CBS/MRCI, the equilibrium distances and angle are within 0.001 Å and 0.2° of experimental values while the available measured vibrational spectra are reproduced to within 11 cm^{-1} rms error. Addition of a CCSD(T) based core-valence correction and a dynamically weighted Davidson correction (based on FCI results at a small basis set level) reduce the rms error to below 2 cm^{-1}. It is likely that our correction benefits from fortuitous cancelation of errors because we have neglected several small high-order corrections. For example, significant contributions from relativistic and non-Born−Oppenheimer effects have been noted for this system.[79]

B. HCN:HNC. ***Fitting Accuracy Tests.*** For our preliminary tests, the Aces II electronic structure code[65] was used to compute

TABLE 2: Computed Vibrational Levels for the Various Theoretical Models Compared with Other Calculations and Experiment

level	ν_1	ν_2	ν_3	MRCI/ CBS[a]	MRCI+Q/ CBS	MRCI/ CBS+CV	MRCI/ CBS+CV+W(Q)	MRCI/ CBS+CV+DW(Q)	Green[b]	Comeau[c]	expt.[d]
CH_2	0	0	0	3602.33	3601.37	3610.65	3610.03	3610.07		3588.4	
1	0	1	0	1357.79	1348.31	1358.66	1352.46	1352.94	1355.3	1339.3	1352.467
2	0	2	0	2676.65	2657.63	2678.21	2665.76	2668.14	2671.4	2638.6	2667.74
3	1	0	0	2798.17	2798.83	2804.64	2805.09	2805.26	2789.8	2787	2806.01
4	0	0	1	2853.97	2858.48	2861.68	2864.62	2864.61	2841.1	2842.8	2864.97
5	0	3	0	3964.45	3932.85	3966.73	3946.10	3953.00	3958.3	3901.6	3950.55
6	1	1	0	4150.39	4141.61	4157.72	4151.97	4153.10	4140.1	4114.6	4152.77
7	0	1	1	4196.43	4192.58	4205.37	4202.83	4203.14		4171.4	
8	0	4	0	5215.09	5167.19	5217.51	5186.34	5201.16		5123.8	5196.57
9	1	2	0	5440.06	5427.83	5449.90	5441.76	5444.65		5387.9	5444.9
10	0	2	1	5484.29	5478.56	5495.75	5491.86	5493.04		5448.3	
11	2	0	0	5519.03	5517.12	5530.55	5529.42	5530.39		5483.5	5531.4
12	1	0	1	5544.97	5544.43	5557.01	5556.74	5557.34		5512.7	
13	0	0	2	5660.37	5667.43	5675.13	5679.71	5679.72		5635.3	
14	0	5	0	6418.98	6348.79	6421.24	6375.69	6404.02		6297.5	6403.0
15	1	3	0	6714.47	6688.94	6724.42	6707.70	6715.11		6629.8	6714.1
16	0	3	1	6765.07	6746.57	6776.71	6764.55	6768.82		6708.5	
17	2	1	0	6857.54	6848.49	6870.65	6864.77	6867.15		6798.4	
18	1	1	1	6876.60	6870.14	6890.45	6886.26	6887.94		6827.5	
19	0	1	2	6990.13	6989.22	7005.81	7005.19	7005.64		6952.1	
20	0	6	0	7550.78	7447.37	7551.66	7484.80	7539.89		7409.2	
21	1	4	0	7946.20	7905.14	7956.51	7929.79	7945.40		7828.4	
22	0	4	1	8008.40	7977.72	8020.84	8000.69	8010.29		7930.4	
23	2	2	0	8060.09	8063.68	8079.19	8081.51	8083.16		8007.1	
24	1	2	1	8072.85	8077.68	8091.95	8095.16	8096.39		8019.3	
25	3	0	0	8172.35	8158.63	8187.44	8178.51	8183.00		8089.4	
26	0	2	2	8189.05	8176.93	8204.52	8196.60	8199.97		8120.3	
27	2	0	1	8250.82	8250.69	8269.76	8269.55	8270.46		8221.7	
28	1	0	2	8326.13	8323.74	8344.07	8342.67	8344.10		8279.9	
29	0	0	3	8379.94	8390.66	8401.56	8408.50	8408.49		8334.6	
30	0	7	0	8547.77	8395.84	8546.82	8448.87	8561.59		8433.1	
CD_2	0	1	0	1010.28	1003.64	1011.07	1006.72	1006.72	1006		1004.8
	0	3	0	2962.69	2943.05	2964.99	2952.12	2952.35			2948.5
MUSE				9.30	15.67	9.26	4.84	1.40	9.7	48.9	
RMSE				10.72	20.78	11.29	8.53	1.95	12.4	56.3	

[a] Methods are MRCI/CBS (complete basis limit MRCI), MRCI+Q/CBS (added Davidson correction), MRCI/CBS+CV (complete basis limit MRCI with added core-valence correction), MRCI/CBS+CV+W(+Q) (addition of weighted (constant) Davidson correction), and MRCI/CBS+CV+DW(+Q) (addition of dynamically weighted Davidson correction). [b] Calculated levels reported by Green et al.[1] [c] Calculated levels reported by Comeau et al.[2] [d] Experimental levels from the compilation by Gu et al.[8]

energies and analytic gradients using the CCSD(T) method (frozen core) and the relatively inexpensive aug-cc-pVDZ basis set.[80] On the basis of the $^1CH_2$ results, we chose Jacobi coordinates instead of bond distances for study of the HCN: HNC system. These were the same coordinates we used in refitting a previously published PES for this system as part of our IMLS developmental work.[42] The fit was done with r (C−N bond distance) ranging from 1.78 bohr to 2.86 bohr, R (distance from H to the center of mass of CN) ranging from 1.34 bohr to 4.50 bohr, and θ (angle between r and R) ranging from 0° to 180°. The total energy was restricted to range 0−35 000 cm^{-1} (~100 kcal/mol). The IMLS fitting basis was the HDMR(12,9,7) basis, the same used for $^1CH_2$. Starting with 304 seed points, and adding sets of eight automatically selected points (one point per parallel processor), convergence was extremely rapid. A plot of the convergence behavior is shown in Figure 5. As in the case of $^1CH_2$, estimated error and true error (see Section 2) closely follow one another. As shown in Figure 5, the true errors (rms and MUSE) are in fact slightly lower than the estimated error. With 440 data points the fitted surface has a true MUSE of 1.0 cm^{-1} over a 35 000 cm^{-1} range. At 488 points the estimated error falls below the 1.0 cm^{-1} accuracy target and the surface generation is terminated. This level of convergence required only ~300 points in the case of $^1CH_2$, but there the energy range is only about half as much (20 000 cm^{-1}) and permutation symmetry doubles the amount of data.

As briefly described in section 2.A and more fully described in Supporting Information, we have developed a more extensive search system for selecting where to place new points when growing an IMLS fit. A possible measure of the efficacy of this search system is to compare the results in Figure 5 with our previous fit to a published surface for this system that was done with a less exhaustive search for optimal data point location. With an identical HDMR fitting basis set, those fits required ~1000 points with energies and gradients to achieve wavenumber accuracy.[42] As described in section 2.A and Supporting Information, the efficacy of our more extensive search systems grows with the number of ab initio points incorporated in the fit. Because the configuration space and thus the required number of ab initio points grows with the number of atoms in the system, our expectation was that the more comprehensive search method may not make a significant difference in efficiency for three-atom systems but would become more important in higher dimensions. It is gratifying that using the new search strategy a fit to real ab initio data for a three-atom system achieved wavenumber accuracy with fewer than half as many points.

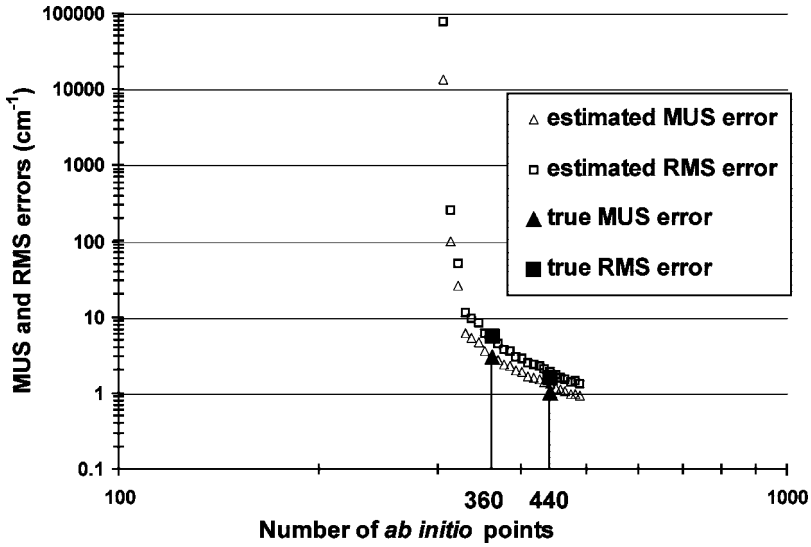

Figure 5. As in Figure 2 but only for HCN and for Jacobi coordinates. True mean unsigned error is subwavenumber at 440 ab initio data points.

High Quality Surfaces: HCN:HNC. Two spectroscopically accurate ab initio PESs have been published for the HCN-HNC system.[19,32] Both were fits to energies computed with the CCSD(T) method and made use of the largest basis sets that could be practically implemented at the time (cc-pCVDZ, cc-pCVTZ, cc-pCVQZ, and cc-pCV5Z in the case of single critical point calculations by van Mourik et al.[32]). van Mourik et al. tried augmented versions of these basis sets for ~20 of the ~250 points for which they calculated energies but decided on cost effectiveness grounds not to pursue these more expensive calculations. The final PES by van Mourik et al. is built upon the earlier one by Bowman et al.[19] via a "morphing" procedure designed to include ab initio data from different basis sets (we designate the van Mourik et al. and Bowman et al. PESs as TvM and JB, respectively). Both publications include vibrational calculations while the van Mourik et al. study includes an extensive treatment of the basis set dependence of the geometries and energies (including CBS extrapolations) of critical points of the system as well as a dipole moment surface (DMS) and relativistic and adiabatic correction surfaces. Van Mourik et al. compare calculated vibration levels for the TvM and JB PESs with 37 experimentally determined levels (33 HCN + 4 HNC). As pointed out by Varandas et al.[33] there are now 49 experimentally determined levels (38 HCN + 11 HNC) below 12 000 cm^{-1}, and we incorporated all of these in our comparisons. Using all of the reported numbers, we calculated MUSE (rms errors) of 11.9 (15.6) and 15.3 (20.1) cm^{-1} relative to experiment for the TvM and JB PESs, respectively. These accurate results were achieved despite Bowman et al. reporting values of the T_1 diagnostic as large as 0.169 (large values can be interpreted to indicate the need to use multireference methods) in some regions of the PES. The TvM PES is composed of fits to mixed data as well as a scaling procedure for even higher quality calculations at the critical points. To isolate and evaluate the performance of the various ab initio methods and different extrapolation schemes, we decided to compute single reference [CCSD(T)] and multireference [MRCI+Q and CASPT2] surfaces at successive fixed levels of ab initio basis sets and thus produce CBS surfaces (note that despite our $^1CH_2$ results, the larger number of electrons in HCN argues for a Davidson correction to the MRCI). Having single source data for each fit and using the IMLS fitting method allowed verifiably subwavenumber accurate fits for each method.

For the CCSD(T) method, the Aces II program was used to compute energies and analytic gradients. Separate fits were performed for the CCSD(T) method (all electrons correlated) with augmented double-, triple-, and quadruple-ζ core-correlation bases (aug-cc-pCVDZ, aug-cc-pCVTZ, and aug-cc-pCVQZ). Three different CBS extrapolation schemes were implemented for the CCSD(T) method. The first (designated CBS_1) was obtained using eq 1 and the augmented core-correlation triple- and quadruple-ζ surfaces. The second (CBS_2) was obtained using eq 2 and all three surfaces. The third (designated CBS_3) was derived from a scheme suggested by Schwenke[81] based on a set of highly accurate data published by Klopper.[82] Schwenke's approach for two basis sets (X_1 and X_2, eq 3) requires a basis set specific parameter, F.

$$E(\infty) = [E(X_2) - E(X_1)]F + E(X_1) \qquad (3)$$

To obtain the value of this parameter for our basis sets, we performed a series of CCSD(T) (with all electrons correlated) calculations on five small systems (N_2, CH_2, H_2O, CO, and HF). The resulting coefficient of $F = 1.525923$ (for eq 3) was determined to extrapolate total energies calculated at the aug-cc-pCVTZ and aug-cc-pCVQZ levels to the CBS limit. Equations 2 and 3 were found to be much more accurate (and close to each other) than eq 1 for extrapolation of CCSD(T) total energies. Thus, we will not discuss CBS_1 further here.

The efficiencies of the fits were again similar to that of the test fit with each surface converging to subwavenumber estimated fitting error with fewer than 500 points. In growing the PESs we initiated the fitting with only a regular-grid of initial data; no prior calculations of any of the critical points were included. Once the fitted PESs were complete, we determined the critical points on the surfaces using a Newton−Raphson algorithm.[83] Separately, using options in Aces II,[65] we performed ab initio optimizations of the critical points. Comparisons of critical points on the fitted surfaces and those from ab initio optimization are given in Table 3. Clearly, once the entire surface is well-converged, the description of important features of the surface is excellent. Both CBS limit calculations produce excellent agreement with experiment for both HCN and HNC and mostly are slightly less than experiment as would be expected from the expectation-value nature of the measurements.

TABLE 3: Basis Set and ab Initio Method Dependence of Critical Point Geometric Parameters for HCN−HNC

method/basis	r_{CH}/a_0	r_{CN}/a_0	r_{NH}/a_0	HCN angle/deg
HCN				
aug-cc-pVTZ/MRCI+Q[a]	2.0163	2.1950		180.000
aug-cc-pVQZ/MRCI+Q[a]	2.0162	2.1886		180.000
CBS/MRCI+Q[b]	2.0161	2.1839		180.000
CBS/MRCI+Q +CV+corr[c]	2.0141	2.1799		180.000
aug-cc-pCVDZ/CCSD(T) [a]	2.0413	2.2176		180.000
ab initio optimization[d]	2.0413	2.2175		180.000
aug-cc-pCVTZ/CCSD(T)[a]	2.0164	2.1874		180.000
ab initio optimization[d]	2.0164	2.1873		180.000
aug-cc-pCVQZ/CCSD(T)[a]	2.0140	2.1811		180.000
CBS_2/CCSD(T)[b]	2.0133	2.1780		180.000
CBS_3/CCSD(T)[b]	2.0128	2.1779		180.000
experiment[e]	2.0135	2.1793		180.000
experiment[f]	2.0141	2.1792		180.000
HNC				
aug-cc-pVTZ/MRCI+Q[a]		2.2246	1.8858	0.000
aug-cc-pVQZ/MRCI+Q[a]		2.2175	1.8827	0.000
CBS/MRCI+Q[b]		2.2123	1.8804	0.000
CBS/MRCI+Q +CV+corr[c]		2.2081	1.8791	0.000
aug-cc-pCVDZ/CCSD(T)[a]		2.2478	1.9012	0.000
ab initio optimization[d]		2.2479	1.9014	0.000
aug-cc-pCVTZ/CCSD(T)[a]		2.2171	1.8840	0.000
ab initio optimization[d]		2.2171	1.8840	0.000
aug-cc-pCVQZ/CCSD(T)[a]		2.2100	1.8810	0.000
CBS_2/CCSD(T)[b]		2.2063	1.8795	0.000
CBS_3/CCSD(T)[b]		2.2063	1.8794	0.000
experiment[g]		2.209	1.878	0.000
saddle point				
aug-cc-pVTZ/MRCI+Q[a]	2.2432	2.2595	2.6379	71.727
aug-cc-pVQZ/MRCI+Q[a]	2.2409	2.2522	2.6325	71.735
CBS/MRCI+Q[b]	2.2391	2.2468	2.6285	71.741
CBS/MRCI+Q +CV+corr[c]	2.2363	2.2424	2.6217	71.656
aug-cc-pCVDZ/CCSD(T)[a]	2.2706	2.2845	2.6635	71.568
ab initio optimization[d]	2.2707	2.2845	2.6654	71.625
aug-cc-pCVTZ/CCSD(T)[a]	2.2405	2.2514	2.6325	71.753
ab initio optimization[d]	2.2409	2.2515	2.6328	71.755
aug-cc-pCVQZ/CCSD(T)[a]	2.2385	2.2444	2.6248	71.677
CBS_2/CCSD(T)[b]	2.2382	2.2409	2.6207	71.619
CBS_3/CCSD(T)[b]	2.2375	2.2408	2.6206	71.633

[a] Critical points located on IMLS-based fitted surfaces (entirely automatically generated, no initial data were provided near critical points). [b] MRCI+Q extrapolated using eq 1. CCSD(T) extrapolated using eq 2 (CBS_2) and eq 3 (CBS_3, see discussion). [c] MRCI+Q extrapolated using eq 1, plus added core-valence, relativistic and NBO corrections (see Discussion). [d] Critical points on fitted surfaces compared with ab initio optimizations using Aces II. [e] Reference 42 in van Mourik et al.[32] [f] Reference 43 in van Mourik et al.[32] [g] Reference 44 in van Mourik et al.[32]

The structures located on the fitted surfaces are in very close agreement to the direct ab initio structures. The largest disagreements are at the saddle point where difference at the aug-cc-pCVDZ basis set level reach ~0.002 a_0 in r_{NH} and ~0.06° in angle. For the saddle point, optimizations on the fitted surfaces were performed to tolerances that would be impractical to achieve during an ab initio optimization. So it is possible that the very slight differences in saddle point structures are due both to differences in the optimization procedures as well as in the fitted vs ab initio surfaces.

Van Mourik et al.[32] calculated all the critical points in Table 3 with the augmented basis set we used and with direct ab initio optimization. Relative to van Mourik et al., the geometries reported in Table 3 (for double-, triple-, and quadruple-ζ bases) are in very close agreement. In addition, the isomerization barrier of 16 692 cm^{-1} determined on the aug-cc-pCVTZ fitted surface is in exact agreement with the direct ab initio optimized isomerization barrier estimate reported by van Mourik et al. for the same basis set. Our CCSD(T)/CBS_2 and CCSD(T)/CBS_3 barriers are 16 830 and 16 829 cm^{-1}, respectively. Van Mourik et al. calculated a single CCSD(T) energy point with a cc-pCV5Z basis set at a basis-set extrapolated saddle point geometry and obtained 16 820 cm^{-1}, in quite close agreement with our CBS CCSD(T) results.

Vibrational calculations were performed using the surfaces at different zeta-levels as well as with the two CBS extrapolated surfaces described above. The DVR calculations were performed in Jacobi coordinates to determine the $l = 0$ and $J = 0$ band origins. Details for the vibrational calculations are given in section 2.B. The calculations are similar to those done for $^1CH_2$ discussed earlier. Tests of our DVR code, using the TvM PES, produced levels in close agreement (<0.1 cm) with those reported by van Mourik et al.[32] The TvM PES is primarily composed of data from the cc-pCVQZ basis, with some even higher level corrections at the critical points. The MUSE (rms error) for computed levels on the TvM surface is 11.9 (15.6) cm^{-1} over 49 experimental levels (including relativistic and adiabatic corrections). Our fit to double-ζ quality data (aug-cc-pCVDZ) did not produce spectroscopically accurate levels (typical errors were hundreds of wavenumbers). Results from the triple-ζ basis (aug-cc-pCVTZ) were much better but not quite as good as those from the TvM PES. As expected, the augmented quadruple-ζ (aug-cc-pCVQZ) results were quite impressive. The MUSE (rms error) over 49 experimentally determined levels (ranging up to more than 12 000 cm^{-1} above the HCN zero-point-energy) was only 6.8 (8.5) cm^{-1}. For the HNC states, Van Mourik et al. concluded that a large basis set was required for an accurate description. While they did incorporate some augmented basis set calculations in the HNC portion of their PES, their mean and rms errors for the HNC states are still, respectively, 18.4 cm^{-1} and 21.3 cm^{-1} over 11 levels. With the aug-cc-pCVQZ basis consistently used throughout, our PES has a MUSE (rms error) of only 3.3 (3.9) cm^{-1} over the 11 HNC levels.

Unfortunately, extrapolation of the CCSD(T) surfaces by either of the two better extrapolation schemes worsened the agreement with experiment significantly. The CBS surface obtained by eq 2 (CBS_2) is slightly better than that created using eq 3 (CBS_3). However, the MUSE (rms error) for levels computed on the CBS_2 surface is still 18.7 cm^{-1} (22.1) compared to 6.8 (8.5) cm^{-1} obtained using the augmented quadruple-ζ surface alone. CBS_3 produced MUSE (rms errors) of 19.1 (22.4) cm^{-1}. This indicates that the aug-cc-pCVQZ results are only fortuitously good, benefiting from some cancelations of errors. The tendency for all-electron CCSD(T) calculations to overshoot experimental frequencies as the CBS limit is approached has been noted in a number of systematic studies of basis set and correlation effects.[84–86]

For each multireference method (CASPT2 and MRCI+Q), two IMLS-based automatically generated PESs were constructed using augmented triple- and quadruple-ζ (aug-cc-pVTZ and aug-cc-pVQZ) bases. The rates of convergence for the four surfaces are very similar to that of the test calculation discussed above (all reaching subwavenumber estimated fitting MUSE with fewer than 500 ab initio points). Extrapolated CBS surfaces were also produced for the two multireference methods using eq 1. A three-point extrapolation was also implemented using eq 2 and incorporating an additional aug-cc-pVDZ surface. Results from this method were found to be slightly less accurate than results obtained using eq 1 and are thus excluded from further consideration.

DVR calculations were performed on these surfaces exactly as in the CCSD(T) cases described above. The CBS/CASPT2 surface produced calculated levels with a mean error relative to the 49 experimental levels of greater than 50 cm^{-1}. Most of the calculated frequencies were *lower* than experimental values,

suggesting a systematic error. As far as the CBS extrapolation, the results were substantially improved by basis set extrapolation using eq 1; the CBS results were significantly better than quadruple-ζ results. While the CASPT2 method has proven useful for kinetics parameters (e.g., energies along reaction paths), these results suggest it is too approximate for vibrational spectroscopy predictions. These results are comparable to those reported by Sabljić et al.[87] where CBS/CASPT2 calculations produced errors of more than 30 cm^{-1} in the fundamentals of ozone.

The MRCI+Q/CBS results were better with a MUSE (rms error) of 15.3 (17.4) cm^{-1} for the 49 experimental levels. This is superior to the CCSD(T)/CBS results, comparable to the accuracy of levels produced by the JB surface[19] but is still significantly worse than the TvM results. The MRCI+Q method produced geometric parameters at the critical points and a barrier in close agreement with other high-level methods (see Table 3). Comparison to experiment is also excellent but uniformly slightly on the high side of measured values. The predicted structures and frequencies were significantly improved relative to experiment by extrapolation using eq 1.

In order to correct for core-valence (CV) correlation effects not included in the MRCI+Q/CBS surface, we computed an additional CCSD(T) frozen core surface using the aug-cc-pCVTZ basis. Thus a CV correction surface was added using the difference between frozen core and all-electron calculations. The CV correction resulted in a huge improvement lowering MUSE (rms error) by nearly a factor of 5 from 15.3 (17.4) uncorrected to 3.2 (4.0) cm^{-1} corrected over the 49 levels. Finally, we added the relativistic and adiabatic correction surfaces of van Mourik et al.[32] This resulted in a slight but significant improvement with the MUSE (rms error) being reduced to 2.5 (3.2) cm^{-1}. As shown in Table 3, the geometric parameters also improved and are closer to experimental results than any of our other calculations. This surface produced a barrier of 16702 cm^{-1}, $\sim$125 cm^{-1} below the TvM and CCSD(T)/CBS values discussed above. The HNC minimum on that surface is 5301 cm^{-1} above the HCN minimum, $\sim$25 cm^{-1} above the TvM value. In other words, relative to the HNC equilibrium, the isomerization barrier on our best surface is $\sim$150 cm^{-1} lower than that on TvM. This would suggest our bending frequencies should be lower and, as shown in Table 4, they are and in better agreement with experiment. No attempt was made to adjust the Davidson correction as in $^1CH_2$ because the necessary FCI calculations are currently impractical for this system.

4. Summary and Conclusions

In this paper, we have reported the most accurate ground-state PESs currently available for $^1CH_2$ and HCN. These surfaces reproduce the experimentally measured equilibrium geometries to within 0.001 Å for the two distances and within 0.2° for the bending angle. The calculated vibrational spectra for $J = 0$ have mean unsigned (rms) errors relative to experiment of 1.4 (2.0) cm^{-1} for $^1CH_2$ and 2.5 (3.2) cm^{-1} for HCN:HCN including levels approaching 12 000 cm^{-1} above the zero-point energy. These automatically generated surfaces are a significant improvement over previous theoretical calculations. At this level of accuracy for HCN at least, relativistic and non-Born−Oppenheimer effects begin to appreciably affect the error.

For $^1CH_2$ this level of accuracy was achieved by a complete basis set extrapolation of augmented triple and quadruple-ζ level calculations using MRCI wave functions, a core-valence correlation correction derived from CCSD(T) calculations with and without frozen cores, and a geometry-scaled Davidson correction where the scaling parameters are set to approximate Full CI calculations at small basis set levels. The complete basis set extrapolation produced significantly more accurate vibrational frequencies than those derived from the quadruple-ζ basis set calculations alone. The straightforward application of the Davidson correction significantly degraded agreement with experiment, an effect previously noted for $^1CH_2$ and expected for few electron systems. The Davidson correction is designed to correct size extensivity errors in MRCI and can approximate the difference between a Full CI energy (which is size extensive) and an MRCI energy. For $^1CH_2$, Full CI calculations were feasible and tests of the Davidson correction led to a simple scaling of the correction with the bend that reduced error at the small basis level. Application of this scaling to the Davidson correction at the CBS level produced our best result of a 2.0 cm^{-1} rms error relative to the 11 known experimental levels. Calculations of relativistic, non-Born−Oppenheimer and other small corrections are beyond the scope of this paper but for water and HCN, these corrections have a scale comparable to or larger than our best rms error with experiment.

For HCN our most accurate results were obtained by calculations exactly analogous to $^1CH_2$ only with a straightforward application of the Davidson correction. While a full CI test of the Davidson correction would have been desirable, HCN is already too large to make such a Full CI calculation feasible for this project. Like $^1CH_2$, the complete basis set extrapolation was important in improving agreement with experiment. Unlike $^1CH_2$, the core-valence corrections were large and quite significantly improved agreement with experiment. Also unlike $^1CH_2$, a relativistic and non-Born−Oppenheimer correction is available for HCN. Application of this correction slightly improved agreement with experiment.

For HCN, several other electronic structure methods were tried. First, CCSD(T) results extrapolated to the complete basis set level by three different schemes were all in noticeably poorer agreement with experiment than the extrapolated Davidson-corrected MRCI results. At the CCSD(T)/aug-cc-pCVQZ level, the agreement with experiment was superior to any MRCI calculation, extrapolated or not. However, the variation with basis set size led the complete basis set extrapolation away from this good agreement with experiment. Second, the much less expensive CASPT2 approximation to MRCI calculations was tried. CASPT2 calculations extrapolated to the complete basis limit using the same basis sets as were used for MRCI+Q calculations produced frequencies in qualitatively poorer agreement with experiment than any of the other approaches we carried out.

The above calculations were feasible because of an efficient and automatic PES fitting scheme that reduced both the number of expensive calculations and the amount of human attention required to produce surfaces with negligible fitting error for eigenstate calculations of the vibrational levels. On the order of 20 different individually optimized surfaces were produced during the course of this work. The fitting procedure we used to accomplish this was the IMLS method that we have been developing for several years. For this study, we interfaced our IMLS code (with some improvements in our fitting methods; see the Supporting Information) with the electronic structure code packages Gaussian, AcesII, and Molpro. With the combined code, we grew fitted PESs over predefined ranges of energy starting with a sparse set of ab initio seed points on a regular grid. A single input file specifies the molecule, the choice of coordinates, the energy range, the ab initio code, and the accuracy target. Running in parallel on eight processors, a usable

TABLE 4: Computed Vibrational Levels (HCN:HNC) Compared to Other Calculations and Experiment

level	ν_1	ν_2	ν_3	CCSD(T)/ AVCQZ[a]	CCSD(T)/ CBS[b]	MRCI+Q[c]	MRCI+Q +CV[d]	MRCI+Q+CV +corr[e]	TvM +corr[f]	expt.[g]
						HCN				
1	0	2	0	1411.63	1413.09	1405.09	1409.93	1409.78	1414.92	1411.42
2	0	0	1	2099.86	2106.21	2091.50	2099.45	2099.11	2100.58	2096.85
3	0	4	0	2807.09	2810.82	2791.39	2801.05	2800.72	2801.46	2802.96
4	1	0	0	3311.13	3315.74	3306.96	3312.55	3311.69	3307.75	3311.48
5	0	2	1	3506.24	3514.72	3490.52	3503.41	3503.02	3510.99	3502.12
6	0	6	0	4179.40	4189.06	4158.26	4173.21	4172.66	4176.24	4174.61
7	0	0	2	4183.21	4192.50	4161.76	4176.60	4175.92	4181.45	4173.07
8	1	2	0	4684.87	4690.54	4673.02	4683.59	4682.63	4686.29	4684.31
9	0	4	1	4895.71	4906.49	4871.34	4888.97	4888.49	4891.76	4888.00
10	1	0	1	5396.80	5407.74	5383.53	5397.15	5395.91	5394.43	5393.70
11	0	8	0	5538.35	5546.75	5506.13	5525.79	5524.98	5537.76	5525.81
12	0	2	2	5579.90	5595.52	5554.69	5574.90	5574.28	5586.50	5571.89
13	1	4	0	6042.11	6049.71	6020.90	6036.31	6035.21	6033.72	6036.96
14	0	0	3	6239.00	6259.24	6211.53	6233.62	6232.62	6242.42	6228.60
15	0	6	1	6265.93	6278.73	6232.90	6255.47	6254.85	6260.59	6254.38
16	2	0	0	6519.55	6528.00	6510.32	6521.78	6520.07	6513.50	6519.61
17	1	2	1	6765.56	6778.23	6744.13	6762.85	6761.63	6768.51	6761.33
18	0	10	0	6871.83	6882.92	6831.98	6856.50	6855.37	6879.60	6855.53
19	0	4	2	6963.30	6981.25	6929.25	6954.43	6953.82	6960.99	6951.68
20	1	0	2	7462.13	7479.95	7439.12	7459.51	7457.92	7461.60	7455.42
21	0	2	3	7632.81	7655.87	7597.30	7624.81	7624.02	7641.28	7620.22
22	2	2	0	7855.14	7864.30	7837.74	7854.29	7852.53	7855.84	7853.51
23	1	4	1	8116.80	8131.41	8079.72	8110.25	8108.98	8110.25	8107.97
24	0	0	4	8278.49	8306.05	8241.28	8270.87	8269.60	8283.37	8263.12
25	0	6	2	8327.36	8347.41	8285.22	8315.39	8314.74	8323.52	8313.53
26	2	0	1	8589.23	8604.08	8571.02	8590.39	8588.27	8584.74	8585.58
27	1	2	2	8825.01	8844.86	8793.71	8819.70	8818.24	8830.27	8816.00
28	0	4	3	9009.61	9035.00	8965.35	8998.18	8997.52	9009.00	8995.22
29	2	4	0	9173.43	9194.90	9146.84	9168.44	9166.58	9164.08	9166.62
30	1	0	3	9507.29	9532.02	9475.08	9503.03	9501.14	9508.91	9496.44
31	3	0	0	9627.67	9639.68	9612.83	9630.61	9628.06	9619.29	9627.09
32	2	2	1	9920.266	9936.36	9893.49	9918.05	9915.98	9922.92	9914.4
33	2	0	2	10638.72	10660.34	10658.80	10635.69	10635.01	10636.7	10631.4
34	0	10	2	10984.18	11016.74	10966.65	10977.26	10976.31	11006.5	10974.2
35	0	4	4	11034.41	11020.22	10980.26	11020.69	11020.04	11035.7	11015.9
36	1	0	4	11526.08	11519.11	11519.26	11527.14	11524.98	11549.6	11516.6
37	0	2	5	11678.79	11709.32	11655.89	11662.04	11661.07	11688.1	11654.59
38	3	0	1	11675.58	11697.21	11677.51	11681.07	11678.08	11672.8	11674.50
						HNC				
1	0	2	0	930.10	932.14	917.02	925.81	925.19	941.92	926.51
2	0	4	0	1875.03	1879.60	1852.28	1869.19	1867.75	1903.10	1873.74
3	0	0	1	2024.16	2030.81	2017.27	2024.73	2024.42	2024.95	2023.88
4	0	2	1	2939.04	2947.90	2925.60	2934.96	2934.11	2955.05	2934.82
5	1	0	0	3656.73	3662.48	3652.79	3658.41	3656.99	3665.10	3652.68
6	0	4	1	3870.57	3882.09	3839.86	3864.66	3863.02	3902.41	3868.35
7	0	0	2	4027.32	4030.02	4013.50	4028.52	4027.89	4029.21	4026.40
8	1	2	0	4531.71	4541.14	4525.41	4540.00	4538.07	4558.11	4534.45
9	1	4	0	5440.87	5450.99	5450.28	5437.90	5433.42	5469.23	5435.66
10	1	0	1	5669.33	5681.62	5658.32	5655.94	5670.31	5676.51	5664.85
11	2	0	0	7179.14	7167.40	7162.48	7170.31	7176.76	7189.47	7171.41
MUSE				6.84	18.71	15.32	3.19	2.53	11.93	
RMSE				8.54	22.14	17.36	3.96	3.19	15.60	

[a] CCSD(T)/aug-cc-pCVQZ. [b] CCSD(T)/CBS, basis extrapolation using eq 3 and fitted PESs at aug-cc-pVDZ, aug-cc-pVTZ, and aug-cc-pVQZ levels. [c] MRCI+Q/CBS, basis extrapolation using eq 1 and fitted PESs at aug-cc-pVTZ and aug-cc-pVQZ levels. [d] MRCI+Q/CBS +CV (with added core-valence correction). [e] MRCI+Q/CBS +CV + Relativistic + non-Born−Oppenheimer corrections by van Mourik et al.[32] [f] Relativistic and non-Born−Oppenheimer corrected surface by van Mourik et al.[32] (VQZANO+) [g] For HCN: refs 1, 2, and 4−6 in van Mourik et al.;[32] for HNC: refs 70 and 71 in van Mourik et al.,[32] and refs 38−43 in Varandas et al.[33]

PES can be produced quickly in a fairly black box fashion. The fitting accuracies of the fitted PESs were confirmed by computing a test set of vibrational levels for $^1CH_2$ using the fitted surface nominally converged to 0.33 cm^{-1} mean unsigned fitting error and using direct ab initio electronic structure calculation of the points required by the DVR vibrational eigenstate program. The mean unsigned and maximum differences for these two eigenstate calculations for all 216 levels below 20 000 cm^{-1} are 0.10 cm^{-1} and 0.41 cm^{-1}, respectively. These errors are consistent with the convergence error of the fit, and they are small relative to errors produced by deficiencies in the electronic structure calculations.

Most of the intellectual effort required to generate highly accurate PES goes into determining an appropriate and reliable scheme for the ab initio electronic structure calculations. Because sophisticated electronic structure methods can have

convergence problems, black box surface fitting can be problematic for interpolation methods (including splines, modified Shepard, and our IMLS-based scheme) that pass exactly through all data points, allowing unconverged data to cause oscillations in the fit. However, this problem can be recognized during a fit using IMLS because the automatic data point selector will start to place a large number of points into a very small region of configuration space. By monitoring the locations of added data, and by examining preliminary surfaces while the fit is ongoing, one can generally ensure that the ab initio calculations are converging properly. In our generation of approximately 20 different surfaces for this work, no unconverged points were detected during the automatic growth of the PESs. Of course, noninterpolative methods are less sensitive to bad points and might therefore require even less human attention. However, such methods are typically less sensitive to all points and typically cannot achieve the level of fitting accuracy displayed here by IMLS methods with so few ab initio calculations.

Acknowledgment. We acknowledge very helpful discussions with Kirk Peterson (Washington State University) that clarified the limitations of different electronic structure methods. We acknowledge helpful discussions with Lawrence Harding and Michael Minkoff (Argonne National Laboratory) in the course of this work. This work was supported by the U.S. Department of Energy, Office of Basic Energy Sciences, Division of Chemical Sciences, Office of Science, U.S. Department of Energy under Contract No. W-31-109-Eng-38 (Argonne) and Contract No. DE-FG02-01ER15231 (UM).

Supporting Information Available: The three-atom L-IMLS code used to automatically generate the potential energy surfaces discussed here is described in more detail in a stand-alone Appendix. The availability of this code is also discussed. This information is available free of charge via the Internet at http://pubs.acs.org

References and Notes

(1) Green, W. H.; Handy, N. C.; Knowles, P. J.; Carter, S. *J. Chem. Phys.* **1990**, *99*, 118.
(2) Comeau, D. C.; Shavitt, I.; Jensen, P.; Bunker, P. R. *J. Chem. Phys.* **1989**, *90*, 6491.
(3) Petek, H.; Nesbitt, D. J.; Ogilby, P. R.; Moore, C. B. *J. Phys. Chem.* **1983**, *87*, 5367.
(4) Feldmann, D.; Meier, K.; Schmiedl, R.; Welge, K. H. *Chem. Phys. Lett.* **1978**, *60*, 30.
(5) Herzberg, G.; Johns, J. W. C. *Proc. R. Soc. London Ser. A* **1966**, *295*, 107.
(6) Jensen, P.; Bunker, P. R. *J. Chem. Phy.* **1988**, *89*, 1327.
(7) Barclay, J. J.; Hamilton, I. P.; Jensen, P. *J. Chem. Phys.* **1993**, *99*, 9709.
(8) Gu, J.-P.; Hirsch, G.; Buenker, R. J.; Brumm, M.; Osmann, G.; Bunker, P. R.; Jensen, P. *J. Mol. Struct.* **2000**, *517*, 247.
(9) Duxbury, G.; McDonald, B. D.; Van Gogh, M.; Alijah, A.; Jungen, C.; Palivan, H. *J. Chem. Phys.* **1998**, *108*, 2336.
(10) Duxbury, G.; Alijah, A.; McDonald, B. D.; Jungen, C. *J. Chem. Phys.* **1998**, *108*, 2351.
(11) Wang, Z.; Kim, Y.; Hall, G. E.; Sears, T. J. *J. Phys. Chem. A* **2008**, *112*, 9248.
(12) Kim, Y.; Hall, G. E.; Sears, T. J. *J. Mol. Spectrosc.* **2006**, *240*, 269.
(13) Komissarov, A. V.; Lin, A.; Sears, T. J.; Hall, G. E. *J. Chem. Phys.* **2006**, *125*, 084308.
(14) Kim, Y.; Komissarov, A. V.; Hall, G. E.; Sears, T. J. *J. Chem. Phys.* **2005**, *123*, 024306.
(15) Kobayashi, K.; Sears, T. J. *Can. J. Phys.* **2001**, *79*, 347.
(16) Kobayashi, K.; Pride, L. D.; Sears, T. J. *J. Phys. Chem. A* **2000**, *104*, 10119.
(17) Gazdy, B.; Bowman, J. M. *J. Chem. Phys.* **1991**, *95*, 6309.
(18) Bentley, J. A.; Bowman, J. M.; Gazdy, B. *Chem. Phys. Lett.* **1992**, *198*, 563.
(19) Bowman, J. M.; Gazdy, B.; Bentley, J. A.; Lee, T. J.; Dateo, C. E. *J. Chem. Phys.* **1993**, *99*, 308.
(20) Lan, B. L.; Bowman, J. B. *J. Phys. Chem.* **1993**, *97*, 12535.
(21) Lee, T. J.; Dateo, C. E.; Gazdy, B.; Bowman, J. M. *J. Phys. Chem.* **1993**, *97*, 8937.
(22) Wu, Q.; Zhang, J. Z. H.; Bowman, J. M. *J. Chem. Phys.* **1997**, *107*, 3602.
(23) Choe, J.; Tipon, T.; Kukolich, S. G. *J. Mol. Spectrosc.* **1986**, *117*, 292.
(24) Burkolder, J. B.; Sinha, A.; Hammer, P. D.; Howard, C. J. *J. Mol. Spectrosc.* **1987**, *226*, 72.
(25) Smith, A. M.; Coy, S. L.; Klemperer, W. *J. Mol. Spectrosc.* **1989**, *134*, 134.
(26) Jonas, D.; Yang, X.; Wodtke, A. *J. Chem. Phys.* **1992**, *97*, 2284.
(27) Maki, A.; Quapp, W.; Klee, S.; Mellau, G. Ch.; Albert, S. *J. Mol. Spectrosc.* **1996**, *180*, 323.
(28) Northrup, F. J.; Bethardy, G. A.; Macdonald, R. G. *J. Mol. Spectrosc.* **1997**, *186*, 349.
(29) Yang, X.; Rogaski, C. A.; Wodtke, A. M. *J. Opt. Soc. Am. B* **1990**, *7*, 1835.
(30) Maki, A.; Mellau, G. Ch.; Klee, S.; Winnewisser, M.; Quapp, W. *J. Mol. Spectrosc.* **2000**, *202*, 67.
(31) Lecoutre, M.; Rohart, F.; Huet, T. R.; Maki, A. G. *J. Mol. Spectrosc.* **2000**, *203*, 158.
(32) van Mourik, T.; Harris, G. J.; Polyansky, O. L.; Tennyson, J.; Csaszar, A. G.; Knowles, P. J. *J. Chem. Phys.* **2001**, *115*, 3706.
(33) Varandas, A. J. C.; Rodriques, S. P. J. *J. Phys. Chem. A* **2006**, *110*, 485.
(34) Gonzalez, C.; Schlegel, H. B. *J. Chem. Phys.* **1989**, *90*, 2154.
(35) Isaacson, A. D. *J. Chem. Phys.* **2006**, *110*, 379.
(36) For example, van Mourik et al. (ref 32) computed these effects and found the root mean square size of the correction to be less than 15% of the root mean square error in the calculations relative to experiment.
(37) Schatz, G. C. *Rev. Mod. Phys.* **1989**, *61*, 669.
(38) Murrell, J. N.; Carter, S.; Frantos, S.; Huxley, P.; Varandas, A. J. C. *Molecular Potential Energy Functions*; Wiley: Toronto, 1984.
(39) Quack, M. *Annu. Rev. Phys. Chem.* **1990**, *41*, 839.
(40) Dawes, R.; Thompson, D. L.; Guo, Y.; Wagner, A. F.; Minkoff, M. *J. Chem. Phys.* **2007**, *126*, 184108.
(41) Guo, Y.; Tokmakov, I.; Thompson, D. L.; Wagner, A. F.; Minkoff, M. *J. Chem. Phys.* **2007**, *127*, 214106.
(42) Dawes, R.; Thompson, D. L.; Wagner, A. F.; Minkoff, M. *J. Chem. Phys.* **2008**, *128*, 084107.
(43) *Approximation Theory*; Lorentz, G. G.; Chui, C. K.; Shumaker, L. L., Eds.; Academic: New York, 1976.
(44) *Approximation Theory and Spline Functions*; Singh, S. P.; Barry, J. H. W.; Watson, B., Eds.; Reidel: Dordrecht, The Netherlands, 1984.
(45) Bowman, J. M.; Bittman, J. S.; Harding, L. B. *J. Chem. Phys.* **1986**, *85*, 911.
(46) Chapman, S.; Dupuis, M.; Green, S. *Chem. Phys.* **1983**, *78*, 93.
(47) Ischtwan, J.; Collins, M. A. *J. Chem. Phys.* **1994**, *100*, 8080.
(48) Jordan, M. J. T.; Thompson, C. K.; Collins, M. A. *J. Chem. Phys.* **1995**, *102*, 5647.
(49) Evenhuis, C. R.; Manthe, U. *J. Chem. Phys.* **2008**, *129*, 024104.
(50) Lorenz, S.; Gross, A.; Scheffler, M. *Chem. Phys. Lett.* **2004**, *395*, 210.
(51) Gassner, H.; Probst, M.; Lauenstein, A.; Hermansson, K. *J. Phys. Chem. A* **1992**, *102*, 4596.
(52) Prudente, F. V.; Acioli, P. H.; Neto, J. J. S. *J. Chem. Phys.* **1998**, *109*, 8801.
(53) Prudente, F. V.; Neto, J. J. S. *Chem. Phys. Lett.* **1998**, *287*, 585.
(54) Brown, D. F. R.; Gibbs, M. N.; Clary, D. C. *J. Chem. Phys.* **1996**, *105*, 7597.
(55) Blank, T. B.; Brown, S. D.; Calhoun, A. W.; Doren, D. J. *J. Chem. Phys.* **1995**, *103*, 4129.
(56) Sumpter, B. G.; Noid, D. W. *Chem. Phys. Lett.* **1992**, *192*, 455.
(57) Raff, L. M.; Malshe, M.; Hagan, M.; Doughan, D. I.; Rockley, M. G.; Komanduri, R. *J. Chem. Phys.* **2005**, *122*, 84104.
(58) Manzhos, S.; Carrington, T., Jr. *J. Chem. Phys.* **2007**, *127*, 014103.
(59) Hollebeek, T.; Ho, T.-S.; Rabitz, H. *Annu. Rev. Phys. Chem.* **1999**, *50*, 537.
(60) Ho, T.-S.; Rabitz, H. *J. Chem. Phys.* **2003**, *119*, 6433.
(61) Czako, G.; Braams, B. J.; Bowman, J. M. *J. Phys. Chem. A* **2008**, *112*, 7466.
(62) Shepler, B. C.; Braams, B. J.; Bowman, J. M. *J. Phys. Chem. A* **2008**, *112*, 9344.
(63) Wang, Y.; Braams, B. J.; Bowman, J. M.; Carter, S.; Tew, D. P. *J. Chem. Phys.* **2008**, *128*, 224314.
(64) Frisch, M. J; Trucks, G. W.; Schlegel, H. B.; Scuseria, G. E.; Robb, M. A.; Cheeseman, J. R.; Montgomery, J. A., Jr.; Vreven, T.; Kudin, K. N.; Burant, J. C.; Millam, J. M.; Iyengar, S. S.; Tomasi, J; Barone, V.; Mennucci, B.; Cossi, M.; Scalmani, G; Rega, N.; Petersson, G. A; Nakatsuji, H.; Hada, M.; Ehara, M.; Toyota; K.; Fukuda, R.; Hasegawa, J.; Ishida, M.; Nakajima,

T.; Honda, Y.; Kitao, O.; Nakai, H.; Klene, M.; Li, X.; Knox, J. E.; Hratchian, H. P.; Cross, J. B.; Bakken, V.; Adamo, C.; Jaramillo, J.; Gomperts, R.; Stratmann, R. E.; Yazyev, O.; Austin, A. J.; Cammi, R.; Pomelli, C.; Ochterski, J. W.; Ayala, P. Y.; Morokuma, K.; Voth, G. A.; Salvador, P.; Dannenberg, J. J.; Zakrzewski, V. G.; Dapprich, S.; Daniels, A. D.; Strain, M. C.; Farkas, O.; Malick, D. K.; Rabuck, A. D.; Raghavachari, K.; Foresman, J. B.; Ortiz, J. V.; Cui, Q.; Baboul, A. G.; Clifford, S.; Cioslowski, J.; Stefanov, B. B.; Liu, G.; Liashenko, A.; Piskorz, P.; Komaromi, I.; Martin, R. L.; Fox, D. J.; Keith, T.; Al-Laham, M. A.; Peng, C. Y.; Nanayakkara, A.; Challacombe, M.; Gill, P. M. W.; Johnson, B.; Chen, W.; Wong, M. W.; Gonzalez, C.; Pople, J. A. Gaussian 03, Revision B.04, Gaussian, Inc., Wallingford, CT, 2004.

(65) Stanton, J. F.; Gauss, J.; Watts, J. D.; Nooijen, M.; Oliphant, N.; Perera, S. A.; Szalay, P. G.; Lauderdale, W. J.; Kucharski, S. A.; Gwaltney, S. R.; Beck, S.; Bernholdt, A. Balková D. E.; Baeck, K. K.; Rozyczko, P.; Sekino, H.; Hober, C.; Bartlett, R. J. ACES II is a program product of the Quantum Theory Project, University of Florida. Integral packages included are VMOL (Almlöf, J.; Taylor, P. R.), VPROPS (Taylor, P.), and ABACUS (Helgaker, T.; Jensen, H. J. Aa.; Jørgensen, P.; Olsen, J.; Taylor, P. R.).

(66) Werner, H.-J.; Knowles, P. J.; Lindh, R.; Manby, F. R.; Schütz, M.; Celani, P.; Korona, T.; Rauhut, G.; Amos, R. D.; Bernhardsson, A.; Berning, A.; Cooper, D. L.; M. Deegan, J. O.; Dobbyn, A. J.; Eckert, F.; Hampel, C.; Hetzer, G.; Lloyd, A. W.; McNicholas, S. J.; Meyer, W.; Mura, M. E.; Nicklaβ, A.; Palmieri, P.; Pitzer, R.; Schumann, U.; Stoll, H.; Stone, A. J.; Tarroni, R.; Thorsteinsson, T. MOLPRO is a package of ab initio programs.

(67) Light, J. C.; Carrington, T., Jr. *Adv. Chem. Phys.* **2000**, *114*, 263.

(68) Lill, J. V.; Parker, G. A.; Light, J. C. *Chem. Phys. Lett.* **1982**, *89*, 483.

(69) Wei, H.; Carrington, T., Jr. *J. Chem. Phys.* **1992**, *97*, 3029.

(70) Echave, J.; Clary, D. C. *Chem. Phys. Lett.* **1992**, *190*, 225.

(71) Li, G.; Hu, J.; Wang, S.-W.; Georgopoulos, P. G.; Schoendorf, J.; Rabitz, H. *J. Phys. Chem. A* **2006**, *110*, 2474, and references therein.

(72) Helgaker, T.; Jorgensen, P.; Olsen, J. *Molecular Electronic Structure Theory*; Wiley: New York, 2000.

(73) Feller, D.; Peterson, K. A.; Crawford, T. D. *J. Chem. Phys.* **2006**, *124*, 054107.

(74) Petek, H.; Nesbitt, D. J.; Darwin, D. C.; Ogilby, P. R.; Moore, C. B.; Ramsay, D. A. *J. Phys. Chem.* **1989**, *91*, 6566.

(75) Shavitt, I.; Brown, F. B.; Burton, P. G. *Int. J. Quantum Chem.* **1987**, *31*, 507.

(76) Bauschlicher, C. W.; Taylor, P. R. *J. Chem. Phys.* **1986**, *85*, 2779.

(77) Bauschlicher, C. W.; Langhoff, S. R.; Taylor, P. R.; Handy, N. C.; Knowles, P. J. *J. Chem. Phys.* **1986**, *85*, 1469.

(78) Bauschlicher, C. W.; Taylor, P. R. *J. Chem. Phys.* **1986**, *85*, 6510.

(79) Harding, M. E.; Vázquez, J.; Ruscic, B.; Wilson, A. K.; Gauss, J.; Stanton, J. F. *J. Chem. Phys.* **2008**, *128*, 114111.

(80) Kendall, R. A.; Dunning, T. H., Jr.; Harrison, R. J. *J. Chem. Phys.* **1992**, *96*, 6796.

(81) Schwenke, D. W. *J. Chem. Phys.* **2005**, *122*, 014107.

(82) Klopper, W. *Mol. Phys.* **2001**, *99*, 481.

(83) Baker, J. *J. Comput. Chem.* **1986**, *7*, 385.

(84) Bauschlicher, C. W.; Partridge, H. *J. Chem. Phys.* **1994**, *100*, 4329.

(85) Csaszar, A. G.; Allen, W. D. *J. Chem. Phys.* **1996**, *104*, 2746.

(86) Peterson, K. A.; Wilson, A. K.; Woon, D. E.; Dunning, T. H., Jr. *Theor. Chem. Acc.* **1997**, *97*, 251.

(87) Ljubiæ, I.; Sabljiæ, A. *Chem. Phys. Lett.* **2004**, *385*, 214.

JP900409R